

PAPER • OPEN ACCESS

## Enhancing gas sensing properties of novel palladium-decorated zinc oxide surface: a first-principles study

To cite this article: Monrudee Liangruksa *et al* 2021 *Mater. Res. Express* **8** 045004

View the [article online](#) for updates and enhancements.

### You may also like

- [The Dependence of Crystal Plane on Hydrogen Sensing Properties of ZnO Bulk Substrates](#)  
Soohwan Jang, Sunwoo Jung and Kwang Hyeon Baik
- [Influence of Size and Density of Au Nanoparticles on ZnO Nanorod Arrays for Sensing Reducing Gases](#)  
C. M. Chang, M. H. Hon and I. C. Leu
- [Electronic properties of graphene-ZnO interface: a density functional theory investigation](#)  
Maryam Fathzadeh, Hamoon Fahravandi and Ebrahim Nadimi



## ECS Membership = Connection

### ECS membership connects you to the electrochemical community:

- Facilitate your research and discovery through ECS meetings which convene scientists from around the world;
- Access professional support through your lifetime career;
- Open up mentorship opportunities across the stages of your career;
- Build relationships that nurture partnership, teamwork—and success!

**Join ECS!**

**Visit [electrochem.org/join](https://electrochem.org/join)**



# Materials Research Express



## PAPER

# Enhancing gas sensing properties of novel palladium-decorated zinc oxide surface: a first-principles study

### OPEN ACCESS

RECEIVED  
9 February 2021

REVISED  
9 March 2021

ACCEPTED FOR PUBLICATION  
15 March 2021

PUBLISHED  
2 April 2021

Original content from this work may be used under the terms of the [Creative Commons Attribution 4.0 licence](#).

Any further distribution of this work must maintain attribution to the author(s) and the title of the work, journal citation and DOI.



Monrudee Liangruksa<sup>1,\*</sup> , Teeraphan Laomettachit<sup>2,3</sup> and Chawarat Siriwong<sup>4,\*</sup>

<sup>1</sup> National Nanotechnology Center (NANOTEC), National Science and Technology Development Agency (NSTDA), Pathum Thani 12120, Thailand

<sup>2</sup> Bioinformatics and Systems Biology Program, School of Bioresources and Technology, King Mongkut's University of Technology Thonburi (KMUTT), Bangkok 10150, Thailand

<sup>3</sup> Theoretical and Computational Physics (TCP) Group, Center of Excellence in Theoretical and Computational Science Center (TaCS-CoE), KMUTT, Bangkok 10140, Thailand

<sup>4</sup> Department of Physics, Faculty of Science, Silpakorn University, Ratchamankha Nai Rd., Nakhon Pathom, 73000, Thailand

\* Authors to whom any correspondence should be addressed.

E-mail: [monrudee@nanotec.or.th](mailto:monrudee@nanotec.or.th) and [siriwong\\_c@su.ac.th](mailto:siriwong_c@su.ac.th)

**Keywords:** gas sensitivity, zinc oxide, surface modification, palladium, first-principles calculations

Supplementary material for this article is available [online](#)

## Abstract

Doping and surface engineering of zinc oxide (ZnO) nanostructures are the practical approach in promoting the gas sensing capabilities. However, the mechanism and the factors that affect such improvement are not well understood. We performed the first-principles based on density functional theory (DFT) calculations to investigate palladium (Pd) decoration on the gas sensing properties of ZnO (0001) surface. Various Pd loading contents on the ZnO surface have been simulated for the resulting sensing capabilities towards a series of gas molecules. The simulations indicate that the modified ZnO surfaces actively interact with the CO and NH<sub>3</sub> gas molecules with great adsorption energies ranging from  $-1.02$  eV to  $-5.56$  eV. Moreover, the most stable structure of the decorated ZnO surface by a three-Pd ring cluster has revealed the drastically enhanced selectivity towards NH<sub>3</sub> gas. Hence, surface decoration by Pd atoms could be an effective approach in promoting gas selectivity and sensitivity.

## 1. Introduction

Various types of hazardous gases, for example, H<sub>2</sub>S, CO, NO<sub>2</sub>, NH<sub>3</sub>, H<sub>2</sub>, and CH<sub>4</sub>, are routinely released from industrial and agriculture sectors or emitted as vehicle exhaust gases. Using or producing these gases causes health hazards and adverse impacts on humans and animals. Therefore fast and sensitive gas detection, as well as quantification of environmentally hazardous gases, is crucial. Among gas sensing materials, metal oxide (MOX) semiconductors have gained significant interests due to their high sensitivity to chemical environments, long lifetime, fast response time, and relatively high sensitivity [1–3]. Besides the distinct properties, it also suffers from several drawbacks, such as background gas effect, low selectivity, and power consumption in high-temperature conditions. The gas sensitivity is associated with the change in the sensing layer's resistance upon adsorption and reaction with the target gas molecules. Doping or functionalizing the surface of different nanostructures has been validated as an effective approach to enhance gas sensing performance [4–16].

Among the various MOXs, ZnO is the most widely used n-type semiconductor material for gas sensing due to its excellent sensing characteristics and good chemical stability. Several ZnO structures have been investigated from the bulk materials to different morphologies of nanostructures due to their intriguing properties at this scale [17–21]. The improved sensing response of ZnO nanostructures is primarily ascribed to the high single crystalline surface along with a large surface area [1, 22, 23]. The high-performance gas-sensing devices, using ZnO nanostructures, were conducted at room temperature for H<sub>2</sub>, NH<sub>3</sub>, NO<sub>2</sub>, N<sub>2</sub>O and ethanol gas detection [9, 11, 20, 21, 24–26]. The electronic conduction of ZnO-based gas sensors was reported to significantly increase

when exposed to ethanol; thus, it exhibited superior sensitivity and fast response to the gas [11, 12]. However, the sensing performance of pristine nanostructured ZnO can be significantly improved by adding and dispersing noble metal nanoparticles as dopants, impurities, sensitizers, or catalysts onto the surface [9, 11, 18, 27, 28]. The most commonly used metals consist of Au, Ag, Pt, and Pd. This strategic approach can effectively improve MOX's gas sensing characteristics, but it unavoidably increases the material cost to some extent. Among the noble metals, Pd is electrochemically more stable than Fe, Co, and Ni, and it is cheaper than Pt [29]. The previous theoretical study showed that Pd-decorated ZnO nanocluster demonstrates the enhanced gas sensitivity towards H<sub>2</sub> detection [30], which agrees with the prior experimental results on Pd-decorated ZnO nanorods [31]. Based on DFT investigations, transition metals such as Pd, Au, Fe, and Co-doped the hexagonal-ZnO exhibited much higher adsorption capacity to H<sub>2</sub>S compared with their undoped counterparts [32]. Combined with the experimental and DFT studies, the Pd-loaded ZnO nanosheets prepared by a facile hydrothermal method exhibited high gas sensing response and selectivity [33]. These enhanced properties are primarily ascribed to the reduced band gaps due to the introduction of Pd atoms into the ZnO nanostructures.

However, despite the research progress made to demonstrate the hexagonal-ZnO nanosheets either by mono-Pd doping or decorating for gas sensors, many challenges remain in terms of attaining the sensing mechanisms, electronic and structural properties of multi-atom modification by Pd atoms. Besides, the studies based on the application of such structure to various hazardous gases were rarely reported. In our previous work [34], the first-principles density functional theory (DFT) calculations were employed to understand gas sensing characteristics of the ZnO surface upon H<sub>2</sub> and C<sub>2</sub>H<sub>5</sub>OH gas adsorption by varying Pd loading contents. The results have demonstrated that the Pd-decorated ZnO surface is a potential material for the gas sensor as it introduces the band gap reduction and also favors the gas adsorption process. Based on such the modified substrate, this present work investigates the gas sensitivity and selectivity of other gas molecules, using first-principles calculations based on DFT. Of great interest are CH<sub>4</sub>, CO, CO<sub>2</sub>, NH<sub>3</sub>, N<sub>2</sub>O, and NO that are mainly used for industrial, environmental, and medical applications. Our computational results could provide a better understanding of the gas sensing characteristics and yield an atomistic insight into the adsorption process of the gases toward the Pd-decorated ZnO surface at the different coverages.

## 2. Computational details

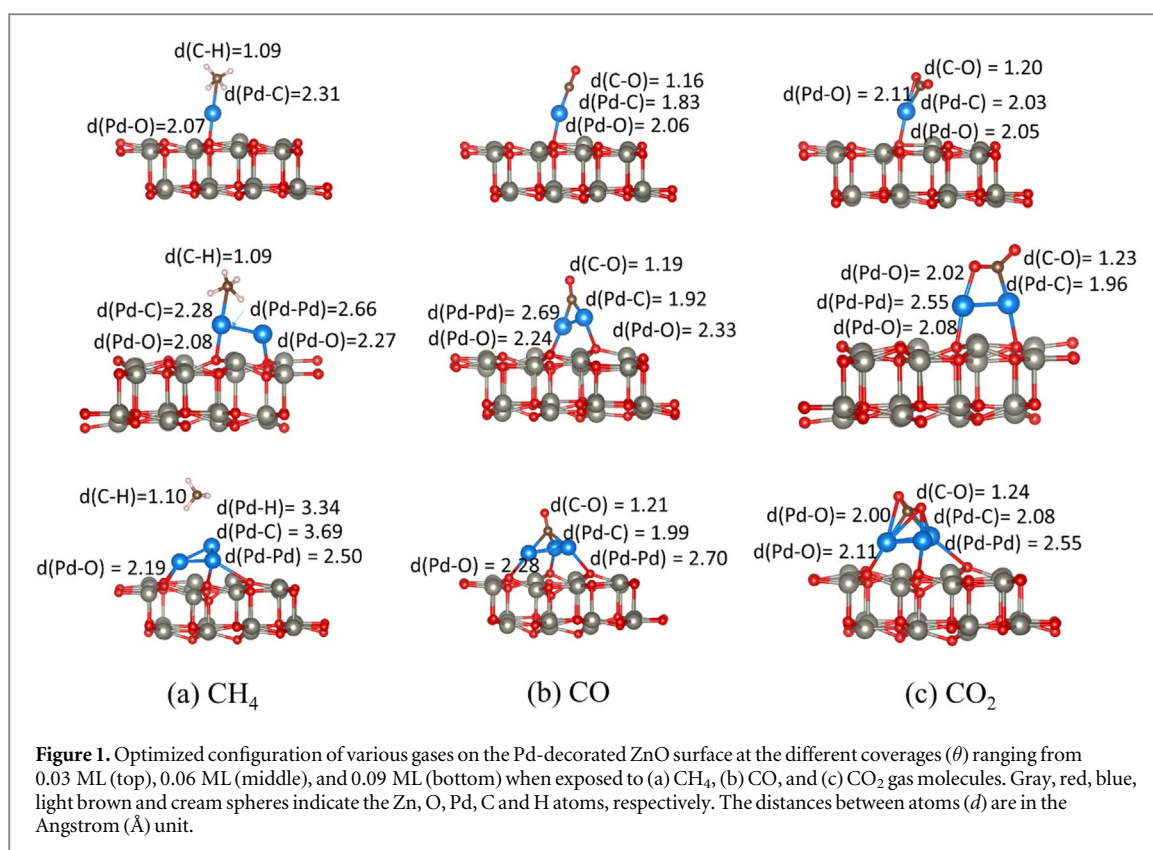
All DFT calculations were done by using the Vienna *ab initio* simulation package (VASP) with a projector augmented wave (PAW) method [35–38]. The electron exchange–correlation interactions were described with a generalized gradient approximation (GGA) in the form of the Perdew–Burke–Ernzerhof (PBE) [39] functional. The van der Waals (vdW) correction proposed by Grimme (DFT-D3) was adopted to take into account the long-range vdW interactions [40, 41]. Throughout this study, we used the cut-off energy for the plane-wave basis expansion of 450 eV, which was adequately high enough to converge the properties of all the pseudopotentials in this work. During relaxations, all atoms' positions were allowed to fully relax until the force on each atom was less than 0.01 eV Å<sup>-1</sup> between two ionic steps, and the convergence of the electronic self-consistent energy was less than 10<sup>-6</sup> eV. The geometry optimization and electronic structure calculations were sampled using the Monkhorst-Pack scheme with (5x5x1) and (9x9x1), respectively. The Bader charge analysis was computed using VASP-VTST [42–44].

It should be noted that the ultrathin ZnO surface consisting of a few layers prefers a graphitic honeycomb as proved by the experiments [45] and first-principles calculations [17, 46–48], in which the Zn and O atoms are coplanar. The ZnO (0001) plane was therefore considered to be the reactive surface in this study. The geometry structures of bare ZnO and Pd-decorated ZnO were optimized following our previous work [34] (see the details in S1 of Supplementary Material available online at [stacks.iop.org/MRX/8/045004/mmedia](https://stacks.iop.org/MRX/8/045004/mmedia)). The polar (0001) and (000 $\bar{1}$ ) surfaces flatten out, forming a new 'graphitic'-like structure as shown in Fig. S1(a). In the z-direction, the vacuum slab of 20 Å was used to avoid the interaction of the close periodical images. The bare ZnO surface was first optimized. Then, the number of Pd atoms varied from one to three atoms as the adsorbates onto the surface, which can be described as the surface coverages ( $\theta$ ) as detailed in S1 of Supplementary Material. The increase in content of Pd-atoms at ZnO [0001] is from 0 Monolayer (ML), 0.03 ML, 0.06 ML, and 0.09 ML, corresponding to the bare ZnO, one, two, and three Pd atoms decorated on the ZnO surface. The binding energy per Pd atom to determine the stability of the Pd-decorated ZnO layer was also shown in S1 of Supplementary Material.

For gas adsorption, various initial sites were employed, which the optimized one with the largest negative  $E_{ads}$  was selected as the stable one. The adsorption energy  $E_{ads}$  is defined as:

$$E_{ads} = E_{sub/gas} - (E_{gas} + E_{sub}), \quad (1)$$

where  $E_{gas}$  and  $E_{sub}$  are energies of the free gas molecule and the substrate (bare ZnO surface or the Pd-decorated ZnO surface, respectively).  $E_{sub/gas}$  denotes the total energy of the combined gas molecule-substrate system.



Noting that stronger force exceeding  $50 \text{ kJ mol}^{-1}$  or  $0.52 \text{ eV}$  are responsible for chemisorption while below that is physical adsorption [49].

### 3. Results and discussion

The geometries of the bare ZnO and Pd-decorated ZnO surfaces as the substrates were investigated in terms of structural properties. More detailed information on the binding energy ( $E_b$ ) of the Pd-decorated ZnO surface is listed in S1 of Supplementary Material.  $E_b$  per Pd atom exhibits the negative values, ranging from  $-1.56 \text{ eV}$ ,  $-1.74 \text{ eV}$ ,  $-2.19 \text{ eV}$  for the surface coverages ( $\theta$ ) of 0.03 ML, 0.06 ML, and 0.09 ML (corresponding to one, two, and three decorating-Pd atoms, respectively). Thus, the simulation results ensure the favorable formation of the Pd-decorated ZnO surface, which  $\theta = 0.09 \text{ ML}$  exhibits the most stable structure due to the largest  $E_b$  of  $-2.19 \text{ eV atom}^{-1}$ . The isolated gas molecules were optimized, which the adsorption lengths and bond angles were listed in Fig. S.1(e) in Supplementary Material. The interactions of the single molecules including, CH<sub>4</sub>, CO, CO<sub>2</sub>, NH<sub>3</sub>, NO, and NO<sub>2</sub> to the modified ZnO surfaces, can be described regarding their structural properties and adsorption energies ( $E_{ads}$ ) based on equation (1). Each gas molecule was initially aligned above the Pd-modified ZnO surface with various orientations, in which the most stable configurations with the largest negative  $E_{ads}$  can be summarized in figures 1 and 3. The adsorption energy, the binding distance, the estimated bandgap, the Fermi level, and the net charge transfer ( $\Delta Q$ ) from Bader charge analysis were listed in table 1.

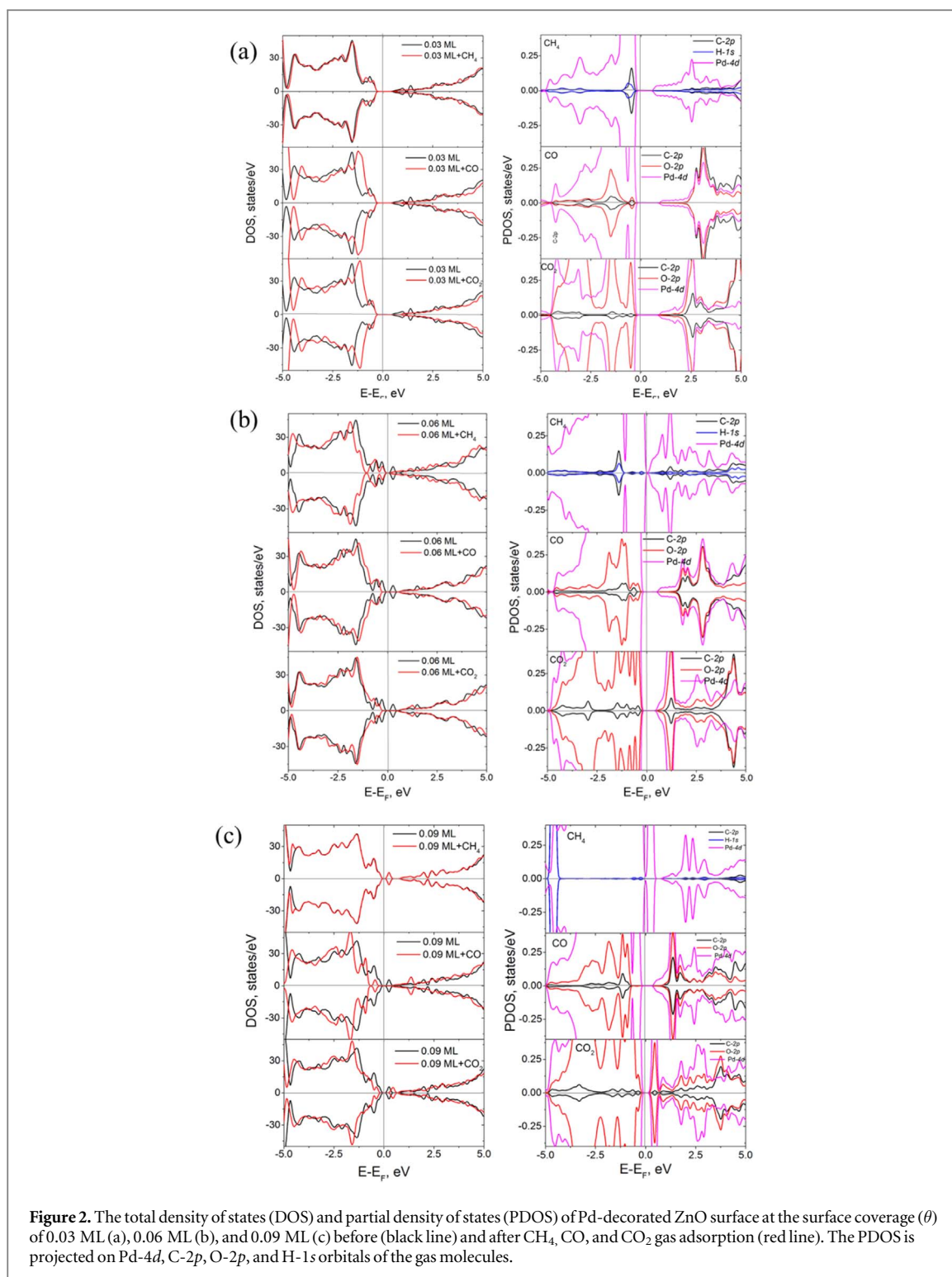
#### 3.1. CH<sub>4</sub> gas adsorption

Upon exposure to CH<sub>4</sub> on the bare ZnO (Fig. S2(a) in Supplementary Material),  $E_{ads}$  exhibits the value of  $-0.30 \text{ eV}$  with the bond distance,  $d(\text{H-O})$ , of  $3.00 \text{ \AA}$ . It is worth mentioning that the  $E_{ads}$  basically consists of the distortion energy of the molecule, distortion energy of the surface, and the interaction energy between the molecule and the surface. Noticeably, the configuration result of Fig. S2(a) distinctly displays the surface distortion, possibly resulting in the main contribution of the computed  $E_{ads} = -0.30 \text{ eV}$ . This explains the conflicting results of  $d(\text{H-O}) = 3.00 \text{ \AA}$  and the  $E_{ads}$  of the bare ZnO exposed to the CH<sub>4</sub> gas molecule. In the case of Pd coverage of 0.03 ML, the gas molecule adopts a small tilted angle of  $13^\circ$  to the Z-direction, as shown in figure 1(a). The C atom of CH<sub>4</sub> is pointing to the Pd atom of the modified ZnO surface. The interaction between the gas and substrate leads to a moderate  $E_{ads}$  of  $-0.72 \text{ eV}$  with the bond length between C of CH<sub>4</sub> and Pd, i.e.,  $d(\text{Pd-C})$  of  $2.31 \text{ \AA}$ , indicating that CH<sub>4</sub> is chemically adsorbed on the surface and the charge transfer ( $\Delta Q$ ) from the gas molecule to the substrate is  $0.0484 e$ . The largest  $E_{ads} = -0.88 \text{ eV}$  of CH<sub>4</sub> on the modified surface is due

**Table 1.** The calculated adsorption energies of various gases on the Pd-modified ZnO surfaces ( $E_{ads}$ ), adsorption length ( $d$ ) defined as the length of nearest atoms of the substrate and the gas molecule, the band gap energy ( $E_g$ ), the charge transfer ( $\Delta Q$ ), and Fermi energy level ( $E_F$ ).

Configuration	$E_{ads}$	$d$ , Å	$E_g$ , eV	$\Delta Q$ , $e$	$E_F$ , eV
bare ZnO					
CH <sub>4</sub>	-0.30	d(H-O(ZnO)) = 3.00, d*(C-H) = 1.10	1.18	-0.0052	-3.20
CO	-0.55	d(C-Zn(ZnO)) = 2.26, d*(C-O) = 1.14	1.21	0.0305	-3.26
CO <sub>2</sub>	-0.42	d(C-O(ZnO)) = 2.94, d*(C-O) = 1.14	1.19	-0.0197	-3.28
N <sub>2</sub> O	-0.34	d(N-Zn(ZnO)) = 2.54, d*(N-N) = 1.15, d*(N-O) = 1.19	1.20	-0.0025	-3.21
NH <sub>3</sub>	-1.06	d(N-Zn(ZnO)) = 2.14, d*(N-H) = 1.02	1.18	0.1139	-3.10
NO	-0.57	d(N-Zn(ZnO)) = 2.38, d*(N-O) = 1.17	0.18	-0.0702	-2.82
1 Pd atom (0.03 ML)					
CH <sub>4</sub>	-0.72	d(Pd-O(ZnO)) = 2.07, d(Pd-C(CH <sub>4</sub> )) = 2.31, d*(C-H) = 1.09	0.81	0.0484	-2.81
CO	-2.68	d(Pd-O(ZnO)) = 2.06, d(Pd-C(CO)) = 1.83, d*(C-O) = 1.16	1.13	-0.1178	-3.32
CO <sub>2</sub>	-0.88	d(Pd-O(ZnO)) = 2.05, d(Pd-C) = 2.03, d(Pd-O(CO <sub>2</sub> )) = 2.11, d*(C-O) = 1.20	1.12	-0.2929	-3.35
N <sub>2</sub> O	-1.36	d(Pd-O(ZnO)) = 2.04, d(Pd-N) = 1.91, d*(N-N) = 1.15, d*(N-O) = 1.21	0.98	-0.1463	-3.05
NH <sub>3</sub>	-1.55	d(Pd-O(ZnO)) = 2.07, d(Pd-N) = 2.08, d*(N-H) = 1.02	0.79	0.1788	-2.57
NO	-1.57	d(Pd-O(ZnO)) = 2.06, d(Pd-N(NO)) = 1.97, d*(N-O) = 1.24	1.02	-0.3367	-2.34
2 Pd atoms (0.06 ML)					
CH <sub>4</sub>	-0.88	d(Pd-O(ZnO)) = 2.08, d(Pd-Pd) = 2.66, d(Pd-C) = 2.28, d*(C-H) = 1.09	0.15	0.0541	-2.30
CO	-3.66	d(Pd-O(ZnO)) = 2.24, d(Pd-Pd) = 2.69, d(Pd-C) = 1.92, d*(C-O) = 1.19	0.77	-0.2129	-2.95
CO <sub>2</sub>	-1.82	d(Pd-O(ZnO)) = 2.08, d(Pd-Pd) = 2.55, d(Pd-O(CO <sub>2</sub> )) = 2.02, d(Pd-C) = 1.96, d*(C-O) = 1.19	0.70	-0.4856	-2.97
N <sub>2</sub> O	-1.80	d(Pd-O(ZnO)) = 2.21, d(Pd-Pd) = 2.76, d(Pd-N) = 1.95, d*(N-N) = 1.19, d*(N-O) = 1.23	0.57	-0.3656	-2.75
NH <sub>3</sub>	-5.56	d(Pd-O(ZnO)) = 2.04, d(Pd-Pd) = 2.59, d(Pd-N) = 2.06, d*(N-H) = 1.03	0.34	0.1670	-2.20
NO	-3.44	d(Pd-O(ZnO)) = 2.17, d(Pd-Pd) = 2.79, d(Pd-N) = 1.89, d*(N-O) = 1.21	1.12	-0.3270	-2.12
3 Pd atoms (0.09 ML)					
CH <sub>4</sub>	-0.01	d(Pd-O(ZnO)) = 2.19, d(Pd-Pd) = 2.50, d(Pd-C) = 3.69, d(Pd-H) = 3.34, d*(C-H) = 1.10	0.31	-0.0152	-2.82
CO	-3.27	d(Pd-O(ZnO)) = 2.28, d(Pd-Pd) = 2.70, d(Pd-C) = 1.99, d*(C-O) = 1.21	0.59	-0.2789	-2.64
CO <sub>2</sub>	-0.82	d(Pd-O(ZnO)) = 2.11, d(Pd-Pd) = 2.55, d(Pd-C) = 2.08, d(Pd-O) = 2.00, d*(C-O) = 1.24	0.38	-0.5964	-2.85
N <sub>2</sub> O	-1.01	d(Pd-O(ZnO)) = 2.25, d(Pd-Pd) = 2.77, d(Pd-N) = 1.98, d*(N-N) = 1.23, d*(N-O) = 1.23	0.51	-0.4821	-2.64
NH <sub>3</sub>	-1.02	d(Pd-O(ZnO)) = 2.11, d(Pd-Pd) = 2.66, d(Pd-N) = 2.05, d*(N-H) = 1.02	0.05	0.1994	-2.26
NO	-2.48	d(Pd-O(ZnO)) = 2.14, d(Pd-Pd) = 2.66, d(Pd-N) = 1.89, d*(N-O) = 1.21	0.20	-0.3255	-2.52

Note: d\* denotes the bond length of the gas molecule, and d(Pd-O(ZnO)) means the adsorption length between the Pd atom and O atom of the ZnO surface.



to the adsorption on the 0.06 ML surface, displaying the  $d(\text{Pd-C}) = 2.28 \text{ \AA}$  (See the middle panel of figure 1(a)). So the gas molecule is anchored with the Pd atom and tilted with an angle of  $79^\circ$  acting to the  $y$ -axis, and  $\Delta Q = 0.0541 e$  transferred from the CH<sub>4</sub> molecule to the substrate. Next, the adsorption mechanism of the CH<sub>4</sub> gas molecule on 0.09 ML reveals the relatively weak interaction of  $E_{ads} = -0.01 \text{ eV}$  and  $d(\text{Pd-C}) = 3.69 \text{ \AA}$ , as shown in figure 1(a) at the below panel and listed in table 1. Therefore, the simulation results obviously suggest that the CH<sub>4</sub> molecule energetically interacts with the ZnO surface coverage of 0.06 ML.

Furthermore, the total density of states (DOS) and partial density of states (PDOS) of CH<sub>4</sub> on the Pd-modified ZnO surface were calculated for comparisons, as shown in figure 2. The contribution of CH<sub>4</sub> is significantly observed in the Pd coverage of 0.06 ML the DOS shifted downward to lower energy levels, resulting in the peaks around the Fermi level and a hybridization between C-2p orbital of CH<sub>4</sub> molecule and Pd-4d

orbitals around  $-7$  eV as shown in PDOS (data not shown). The levels become partially occupied due to some electrons transferred from the gas to the substrate ( $\Delta Q = 0.0541 e$ ). Meanwhile, the DOS of  $\text{CH}_4$  on  $\theta = 0.03$  ML and  $0.09$  ML are barely altered from the bare ZnO; thus, these surfaces are not sensitive to the presence of  $\text{CH}_4$  gas molecule. Additionally, the estimated bandgap ( $E_g$ ) of  $\theta = 0.06$  ML exhibits the smallest value of  $0.15$  eV, compared to that of bare ZnO ( $E_g = 1.18$  eV),  $\theta = 0.03$  ML ( $E_g = 0.81$  eV), and  $\theta = 0.09$  ML ( $E_g = 0.31$  eV) upon  $\text{CH}_4$  gas adsorption as listed in table 1. It should be noted that  $E_g$  is a crucial factor determining the electrical conductivity ( $\sigma$ ) of a material, which can be written as follows [50]:

$$\sigma \propto \exp\left(\frac{-E_g}{2k_B T}\right), \quad (2)$$

So,  $\sigma$  is exponentially dependent on the negative value of  $E_g$ , where  $k_B$  denotes the Boltzmann's constant, and  $T$  is the temperature. The sensitivity  $S$  can be defined as  $S = R_a/R_g$ , where  $R_a$  is the resistance in ambient air, and  $R_g$  is the resistance in the air-mixed gas. This can also be written as:

$$S = R_a/R_g \text{ or } S \propto \exp\left(\frac{E_{g0} - E_{g1}}{k_B T}\right), \quad (3)$$

where  $E_{g1}$  is the bandgap of the ZnO surface or the Pd-modified ZnO surface upon gas adsorption, and  $E_{g0}$  is the bandgap of the bare ZnO surface or the Pd-decorated ZnO surface without gas adsorption. Hence, the sensitivity will grow exponentially with a decrease in the bandgap energy ( $E_{g0} > E_{g1}$ ) when exposed to the gas molecule. Based on equations (2) and (3), it can be expected that the Pd coverage of  $0.06$  ML could convert the presence of  $\text{CH}_4$  to the electrical signal better than other surfaces.

### 3.2. CO gas adsorption

On the bare ZnO, the most stable adsorption site for CO is located above the Zn atom of the ZnO surface and tilted to the substrate surface (See Fig. S2(b) of Supplementary Material). From table 1,  $E_{ads}$  is calculated to be a moderate value of  $-0.55$  eV, while the adsorption length between C atom of CO and Zn atom of ZnO or d(C-Zn) is  $2.26$  Å. The charge transferred from CO to the ZnO surface is  $0.0305 e$ . This indicates that the interaction of CO with the ZnO surface involves chemisorption. Similar behaviors are also presented in the Pd-decorated ZnO surface upon CO exposure but with a relatively more robust interaction. On  $\theta = 0.03$  ML, the adsorption site of the CO molecule is shown in figure 1(b). The C-O bond is tilted toward the surface, forming an angle of  $<78^\circ$  to the Y-axis with  $E_{ads} = -2.68$  eV, d(Pd-C) =  $1.83$  Å,  $\Delta Q = -0.1178 e$ . Meanwhile, the interaction of CO with  $\theta = 0.09$  ML also shows the relatively stable chemisorption with  $E_{ads} = -3.27$  eV, d(Pd-C) =  $1.99$  Å,  $\Delta Q = -0.2789 e$ . Among these, the CO molecule undergoes the most considerable chemical interaction with  $\theta = 0.06$  ML, yielding  $E_{ads} = -3.66$  eV, d(Pd-C) =  $1.92$  Å,  $\Delta Q = -0.2129 e$ . Noting that the negative sign of  $\Delta Q$  represents the charge transferred from the Pd-modified ZnO or pure ZnO surfaces towards the gas molecule.

All DOS levels of  $\theta = 0.03$  ML and  $0.06$  ML slightly move towards higher energy after CO adsorption, as illustrated in figure 2. As a result, their DOS alter around the Fermi levels, and the  $E_g$  values diminish to  $1.13$  and  $0.77$  eV, respectively. However, the DOS levels of CO adsorbed on  $0.09$  ML shift towards lower energy, in which the  $E_g$  drastically decreases to  $0.59$  eV. Obviously, the Pd-modified ZnO surface upon CO gas adsorption could convert to the electrical signal according to the reduced  $E_g$ ; thereby increasing the  $S$  in equation (3). In terms of PDOS, the hybridization between Pd- $4d$  and C- $2p$  orbitals of CO molecule is observed for all the modified ZnO surfaces, indicating the strong chemical bonds (See PDOS in figure 2).

### 3.3. CO<sub>2</sub> gas adsorption

The most energetically favorable configurations for  $\text{CO}_2$  adsorption on the bare ZnO and the Pd-decorated ZnO surfaces are shown in Fig. S2(c) in Supplementary Material and figure 1(c). The bare ZnO surface demonstrates d(C-O) =  $2.94$  Å between the C atom of  $\text{CO}_2$  and O atom of ZnO, and  $\Delta Q$  is  $-0.0197 e$ , even if the  $E_{ads}$  is  $-0.42$  eV. Like the bare ZnO upon  $\text{CH}_4$  gas adsorption, the main contribution of  $E_{ads}$  is perhaps derived from the structural deformation energy, which can be obviously seen from figure S2(c). Thus, the bare ZnO surface is not sensitive to the  $\text{CO}_2$  gas molecule based on the far d(C-O). On the other hand,  $\text{CO}_2$  exhibits robust interaction with  $\theta = 0.06$  ML due to the relative large  $E_{ads} = -1.82$  eV, d(Pd-C) =  $1.96$  Å, and  $\Delta Q = -0.4856 e$ , indicating that  $\text{CO}_2$  molecule acts as an electron acceptor. The optimized configuration in figure 1(c) of  $\theta = 0.06$  ML with  $\text{CO}_2$  adsorption clearly shows that  $\text{CO}_2$  is anchored with the two decorated Pd atoms, which one Pd atom binds with C of  $\text{CO}_2$  and the other Pd atom binds with O of  $\text{CO}_2$ . While the coverages of  $0.03$  ML and  $0.09$  ML demonstrate the relatively weaker chemical interaction with the  $\text{CO}_2$  molecule with  $E_{ads} = -0.88$  and  $-0.82$  eV, respectively. The corresponding d(Pd-C) =  $2.03$  Å and  $2.08$  Å, and  $\Delta Q = -0.2929 e$  and  $-0.5964 e$ , representing the charge transferred from the  $0.03$  ML and  $0.09$  ML substrates to the gas molecule, accordingly.

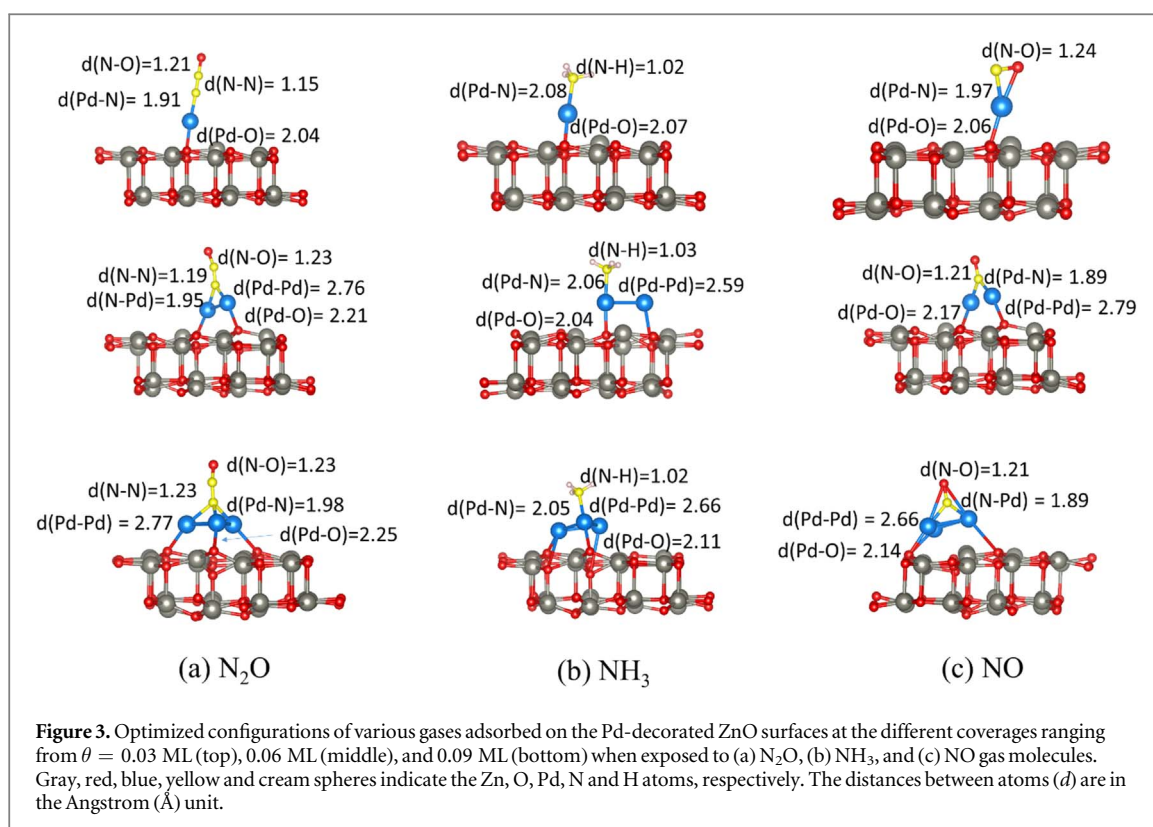
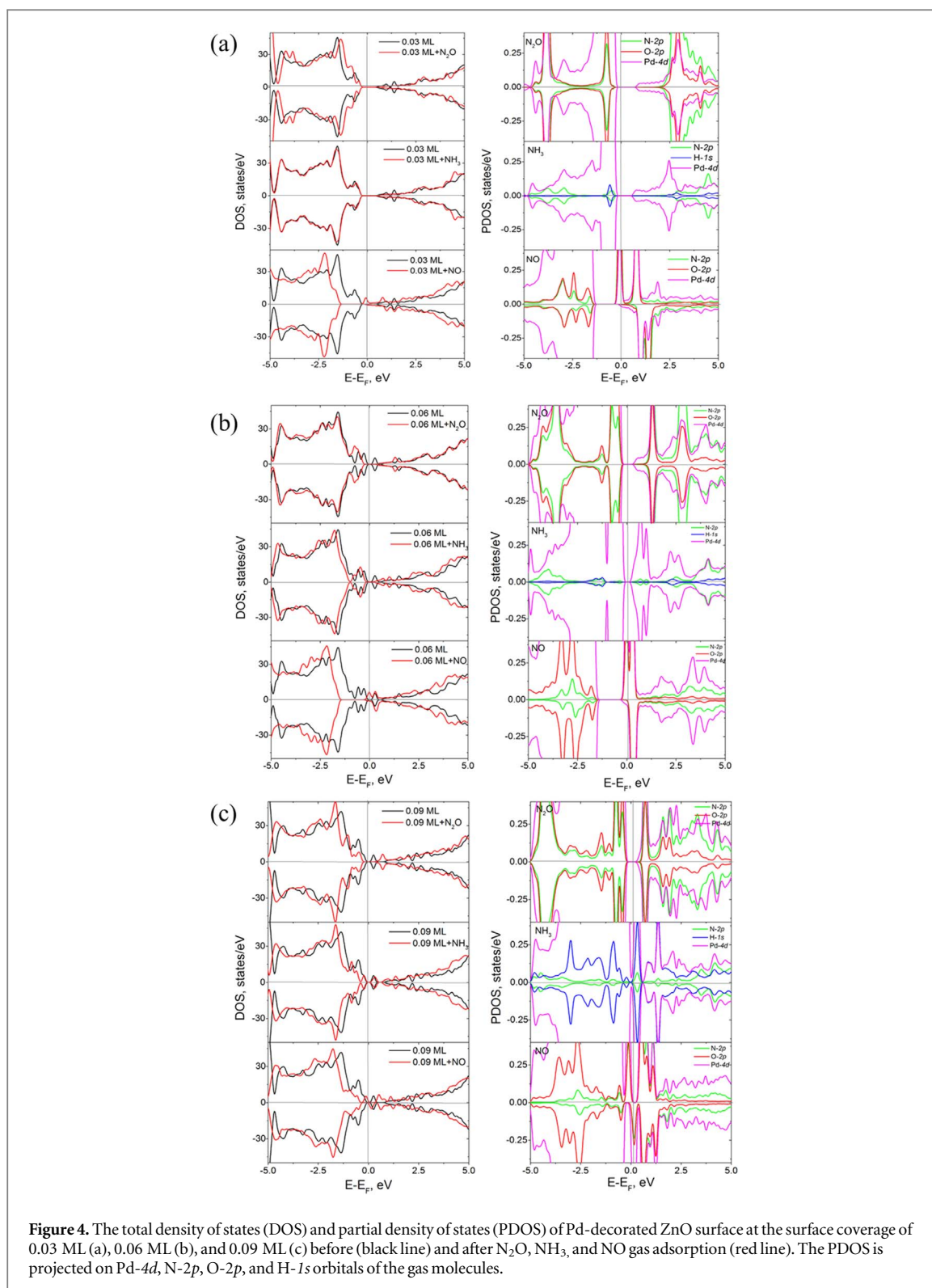


Figure 2 depict DOS and PDOS of the Pd-modified surface upon the CO<sub>2</sub> exposure, while that of the bare ZnO is presented in Fig. S3. It is found that the states of  $\theta = 0.03$  ML are shifted to higher energy levels on account of the relatively strong interaction with the gas molecule. The hybridization of Pd-4*d*, C-2*p*, and O-2*p* orbitals is found between  $-2$  eV to  $-6$  eV in the valence band (See figure 2(a)). Additionally, there are no large shifts observed in the case of  $\theta = 0.06$  ML under the gas adsorption except the small peaks around the Fermi level. However, the hybridization of such orbitals can be noticed around  $-6$  eV (data not shown). The DOS of CO<sub>2</sub> adsorbed on  $\theta = 0.09$  ML have distinct changes in comparison with that of the bare ZnO (See figure 2(c)). Its bandgap is reduced to 0.38 eV due to the small peaks around the Fermi level. The orbital hybridization of Pd-4*d* and C-2*p* and O-2*p* of PDOS can be seen, suggesting the chemical bonding between the gas molecule and substrate.

### 3.4. N<sub>2</sub>O gas adsorption

The most stable adsorption configurations of N<sub>2</sub>O on the bare ZnO and Pd-decorated ZnO surfaces are illustrated in Fig. S2(d) of Supplementary Material and figure 3. The adsorbed molecule aligns straight and is tilted toward the substrate in the x-direction with an angle around 36°. The N atom of N<sub>2</sub>O is anchored with the Zn atom of the bare ZnO, while it is adsorbed to the Pd atom for the modified ZnO surface. The simulation results further suggest that the N<sub>2</sub>O molecule is physisorbed on the bare ZnO surface according to the  $E_{ads} = -0.34$  eV,  $d(\text{N-Zn}) = 2.54$  Å, and  $\Delta Q = -0.0025 e$ , indicating the charge transferred from the surface to the gas molecule. On various surface coverages by Pd atoms, it is found that the gas molecule is strongly bonded with the surface according to the computed  $E_{ads}$  in the range of  $-1.02$  eV to  $-1.80$  eV and  $d(\text{Pd-N})$  from 1.91 Å to 1.98 Å. Meanwhile, the charge transfer is from the substrate to the N<sub>2</sub>O molecule with the most extensive  $\Delta Q = -0.4821 e$  for the  $\theta = 0.09$  ML.

The DOS of N<sub>2</sub>O adsorbed on the bare ZnO surface in Fig. S3 of Supplementary Material has altered near the Fermi level, and the  $E_g$  decreases to 1.20 eV (See table 1), resulting in the electrical conductivity change. The hybridization between N-2*p* orbitals of N<sub>2</sub>O molecule and Zn-4*s* orbital of the ZnO surface is observed around  $-5$  eV and  $-8$  eV, as shown in Fig. S3(b). The DOS levels of  $\theta = 0.03$  ML slightly move toward the higher energy after N<sub>2</sub>O adsorption owing to the charge transfer from the substrate to the gas molecule (see figure 4). On the other hand, the shape of DOS after the adsorption of N<sub>2</sub>O on  $\theta = 0.06$  ML is not changed from that without the gas adsorption as shown in figure 4, except the small peaks around  $-1$  eV below the Fermi level. As  $\theta$  increases to 0.09 ML depicted in figure 4, the DOS levels shift to the lower energy. The  $E_g$  diminishes to 0.51 eV, which could tremendously affect the electrical conductivity and the resulting gas sensing properties.



### 3.5. $\text{NH}_3$ gas adsorption

On the bare ZnO, the  $\text{NH}_3$  molecule is tilted with an angle around  $32^\circ$  to the z-direction and bonded to Zn atom of ZnO with  $E_{ads} = -1.06$  eV, and  $d(\text{Zn-N}) = 2.14$  Å. This indicates the chemical interaction with a large  $\Delta Q = 0.1139 e$  from the  $\text{NH}_3$  gas molecule to the surface. Also, the  $\text{NH}_3$  molecule is chemically adsorbed on the Pd-decorated ZnO surface, exhibiting the  $E_{ads} = -1.55$  eV,  $-5.56$  eV, and  $-1.02$  eV for  $\theta = 0.03$  ML, 0.06 ML, and 0.09 ML, respectively. The corresponding  $d(\text{Pd-N})$  is 2.08 Å, 2.06 Å, and 2.05 Å, accordingly. Similarly, the N atom of  $\text{NH}_3$  prefers to anchor on the Pd-decorating atom with the tilted orientation, as shown in figure 3(b). The direction of charge transfer is from the  $\text{NH}_3$  toward the modified ZnO substrate, in which the dramatic  $\Delta Q = 0.1994$  is found on the Pd coverage of 0.09 ML (see table 1).

Figure 4 depicts the DOS and PDOS of the Pd-decorated ZnO surface upon the gas adsorption. In the case of  $\theta = 0.03$  ML (figure 4(a)), the DOS with and without  $\text{NH}_3$  gas adsorption indicate negligible changes. Unlike, the DOS levels of  $\theta = 0.06$  ML (figure 4(b)) and  $0.09$  ML (figure 4(c)) upon  $\text{NH}_3$  adsorption are shifted downward to lower energy levels, inferring  $\text{NH}_3$  acts as an electron donor. Some peaks occur around the Fermi level, mainly caused by Pd-4d and N-2p of  $\text{NH}_3$  orbital hybridization. As a result, the  $E_g$  of the modified surface upon the gas adsorption decreases from that of bare ZnO surface, i.e.,  $0.79$  eV,  $0.34$  eV, and  $0.05$  eV for  $\theta = 0.03$  ML,  $0.06$  ML, and  $0.09$  ML, respectively. These changes in DOS strongly affect the corresponding electronic properties and can be beneficial for sensing applications. Based on these facts, it is evident that the  $\text{NH}_3$  gas molecule is sensitive to all the modified surfaces and the bare ZnO surface, owing to the relatively large  $E_{ads}$ , small  $E_g$ , and large  $\Delta Q$ .

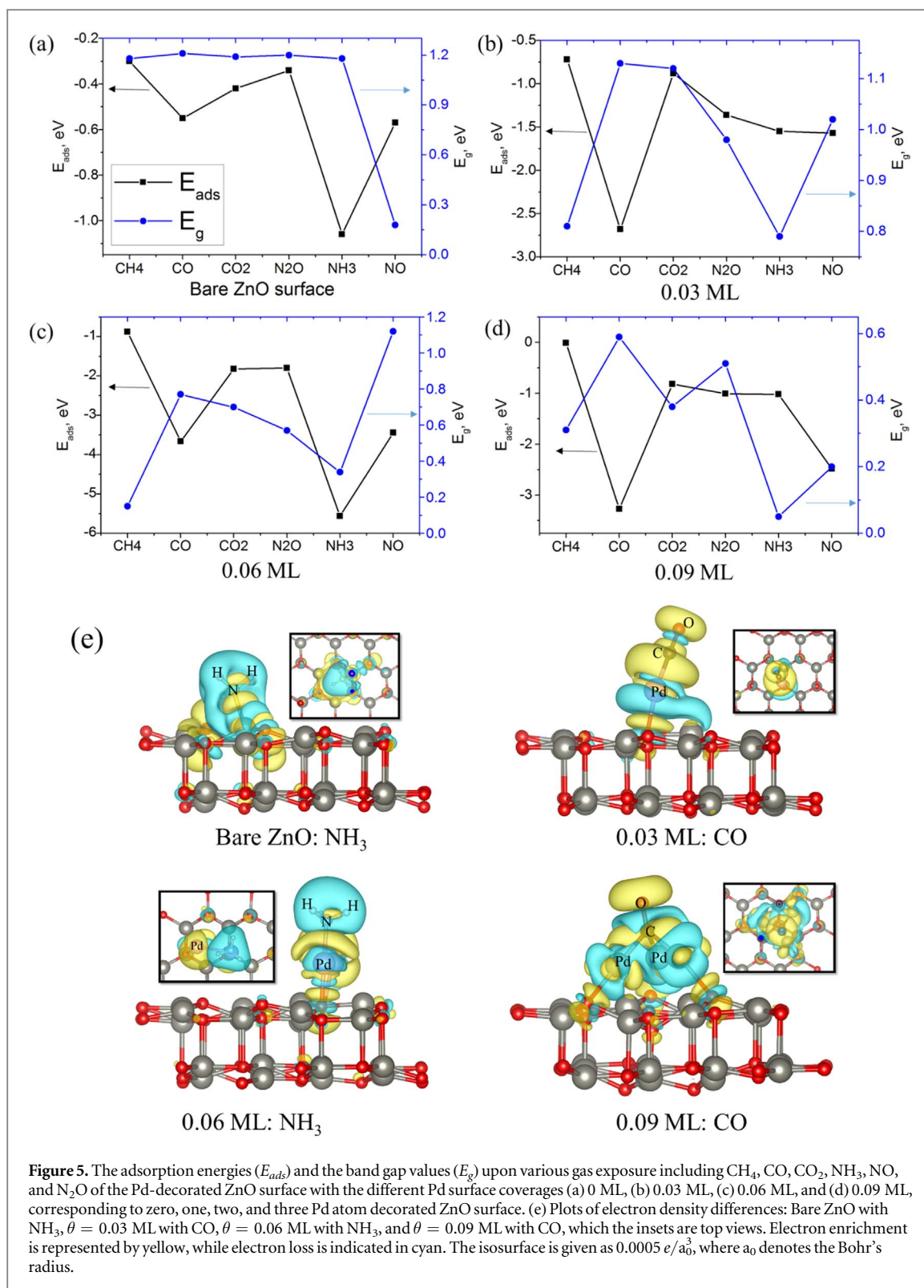
### 3.6. NO gas adsorption

Figure S2(f) of Supplementary Material depicts the optimized of NO molecule on the bare ZnO surface. The  $E_{ads}$  is computed to be  $-0.57$  eV with  $d(\text{Zn-N})$  is  $2.38$  Å, suggesting the moderate interaction. The gas adsorption on the modified ZnO surface is illustrated in figure 3(c). Among these, NO is located on top of Pd with the N-O bond nearly parallel to the  $0.03$  ML surface with the  $E_{ads} = -1.02$  eV and the  $d(\text{Pd-N}) = 1.97$  Å, indicating the strong interaction (See figure 3(c) and table 1). Meanwhile, N of NO molecule prefers to anchor with Pd and align upward to the  $0.06$  ML and  $0.09$  ML surfaces, as shown in figure 3(c), where their corresponding  $E_{ads}$  values are  $-3.44$  eV with  $d(\text{Pd-N}) = 1.89$  Å and  $-2.48$  eV with  $d(\text{Pd-N}) = 1.89$  Å, respectively. It should be noted that the dramatic  $\Delta Q$  is from the modified ZnO surface to the gas (NO),  $\sim 0.3 e$ , demonstrating the changes in the local electronic structure. To further confirm the electrical property, the DOS and PDOS of the modified ZnO surfaces are computed and plotted in figure 4 and S4 of Supplementary Material. Similarly, it is found that NO adsorption has largely modified DOS's shape, in which all the levels are shifted to the lower energy. This can be referred to as that NO is an electron acceptor, receiving the charges from the substrate. Additionally, the values  $\Delta Q$  in table 1 for NO adsorption ensure the charge transfer direction and amount. There is a peak occurring below the Fermi level, about  $-7$  eV and  $-8$  eV (data not shown), mainly caused by Pd-4d orbitals and N-2p orbitals of NO. The peaks observed around the Fermi level due to the level shift bring about considerable changes in electronic properties and the subsequent sensing properties.

Figure 5 depicts  $E_{ads}$  of the bare ZnO and Pd-decorated ZnO surfaces upon various gas exposure, including  $\text{CH}_4$ , CO,  $\text{CO}_2$ ,  $\text{NH}_3$ , NO, and  $\text{N}_2\text{O}$ . As a result, there is no doubt that the Pd-decorated ZnO surface exhibits a relatively higher adsorption tendency than the pure ZnO surface. In the case of pure ZnO, the most stable configuration is due to  $\text{NH}_3$  adsorption ( $E_{ads} = -1.06$  eV). Meanwhile, the other five gases are weakly adsorbed on the surface with the lower  $E_{ads}$  ranging from  $-0.30$  eV to  $-0.57$  eV. Besides, simulation results suggest that CO and  $\text{NH}_3$  are chemisorbed on the Pd-modified ZnO surface. CO exhibits the largest negative  $E_{ads}$  to interact with the Pd coverages of  $0.03$  ML ( $E_{ads} = -2.68$  eV) and  $0.09$  ML ( $E_{ads} = -3.27$  eV). Meanwhile,  $\text{NH}_3$  shows the largest  $E_{ads}$  with the  $0.06$  ML surface ( $E_{ads} = -5.56$  eV). Based on this fact, it can be noticed that the  $\theta = 0.06$  ML is the most reactive surface to the  $\text{NH}_3$  gas molecules owing to the most substantial negative  $E_{ads}$  in comparison with other surfaces. However, too high  $E_{ads}$  is not desired for an efficient sensing mechanism for a reusable sensor. Instead, the gas adsorption should be between physical and weak chemisorption. Moreover, the critical factor affecting the sensitivity (S) is  $E_g$  as listed in equation (3) and figure 5. Therefore, the bare ZnO would be suggested for NO,  $\theta = 0.03$  ML for  $\text{NH}_3$ ,  $\theta = 0.06$  ML for  $\text{CH}_4$ ,  $\text{N}_2\text{O}$ ,  $\text{CO}_2$ , and  $\theta = 0.09$  ML for  $\text{NH}_3$  gas adsorption. Based on the structural stability, the  $0.09$  ML surface shows the most stable formation in terms of the largest negative  $E_b$  per atom, as shown in the S.1 of the Supplementary Material. This can conclude that this surface is suitable to detect the  $\text{NH}_3$  gas molecule because of the  $E_b$ ,  $E_{ads}$ , and small  $E_g$ . The highly sensitive surfaces to the gas molecules in terms of large  $E_{ads}$  and small  $E_g$ , as illustrated in figure 5(e), are suitable for disposable gas sensors. Because the modified ZnO surface at varied coverages can respond to the gases differently, it is possible to apply it for a smart gas sensing device to characterize a unique set of signals from gases by machine learning techniques.

It should also be worth mentioning the underestimation of computed  $E_g$  values by the PBE method. Alternatively, hybrid density functional, Heyd-Scuseria-Ernzerhof, or HSE06 based on a screened Coulomb potential for the nonlocal Hartree-Fock-type exchange interaction was usually adopted to obtain a good approximated  $E_g$ . For example, the HSE06 bandgap of the single-layer- $\text{Ti}_2\text{O}$  is larger than that calculated value using the PBE by  $0.65$  eV [51]. Therefore, although the predicted  $E_g$  by PBE method is lower than the actual values and HSE06, it should not significantly affect the relative comparison of  $E_g$  and their corresponding sensitivity.

To further understand the bonding of this adsorption, the electronic charge density difference is computed to illustrate how the charge change during the adsorption process. The isosurfaces of the charge density differences of the potential gas detection can be calculated using:  $\Delta\rho = \rho_{total} - \rho_{sub/gas} - \rho_{gas}$ , where



$\rho_{total}$ ,  $\rho_{sub/gas}$ , and  $\rho_{gas}$  are the charge densities of the whole system, the substrate with gas adsorption, and the gas molecule, respectively. The corresponding electron density differences of the optimized configurations with the largest  $E_{ads}$  from figures 5(a)–(d) on each surface are selected and plotted in figure 5(e), including  $\theta = 0$  ML, 0.03 ML, 0.06 ML, and 0.09 ML. The simulations suggest that the surfaces are susceptible to NH<sub>3</sub> and CO gas adsorption. It can be seen that Pd-decorating atoms act as the electron acceptor illustrated in yellow (electron enrichment), receiving electrons from the gas molecules. While H atoms of NH<sub>3</sub> exhibit the charge depletion region, and O atom of CO shows the charge accumulation region. Noticeably, the electrons are mainly localized within the bonds rather than around the interface, demonstrating the strong chemical bonding.

## 4. Conclusions

The first-principles calculations based on DFT have been performed to study the gas sensitivity and selectivity of the Pd-decorated ZnO surface under various gas exposure. The influence of surface coverages ( $\theta$ ) by Pd loading is found to significantly promote the gas response, compared to the bare ZnO. The gas sensitivity characteristics are primarily ascribed to the surface modification and its resulting electron transfer mechanism, DOS, bandgap, and gas adsorption. Based on the simulations, CO and NH<sub>3</sub> show considerable gas adsorption to the modified ZnO surfaces, indicating that the surface is significantly sensitive to these gas molecules. A potential gas sensing material should also exhibit a weak chemisorption so that the gas is easily desorbed for the reusable purpose. Thus, each surface variedly interacts with the gas molecules in terms of the crucial factors of band gap reduction and the favorable gas adsorption process. Among the various gas types, the favorable structural formation ( $\theta = 0.09$  ML) indicates the enhanced sensing properties for NH<sub>3</sub> gas detection. The present study's calculations could provide a basic understanding and atomistic insight on the influence of surface modification of ZnO regarding the sensing characteristics and mechanisms upon various hazardous gas exposure. Moreover, the findings could make a prominent contribution to the design of state-of-the-art gas sensing materials with exceptional selectivity and sensitivity.

## Acknowledgments

The authors acknowledge the Nanoscale Simulation Research Team of NANOTEC and NSTDA Supercomputer Center (ThaiSC) for providing computing resources.

## Data availability statement

The data that support the findings of this study are available upon reasonable request from the authors.

## Authors' contributions

ML conceived the presented idea, designed, performed the calculations, and conducted the data analysis. ML and TL interpreted the results and wrote the manuscript. ML, TL, and CS edited the manuscript.

## Declaration of competing interest

The authors declare no competing interest.

## ORCID iDs

Monrudee Liangruksa  <https://orcid.org/0000-0002-7579-9502>

## References

- [1] Dey A 2018 Semiconductor metal oxide gas sensors: a review *Materials Science and Engineering: B* **229** 206–17
- [2] Phanichphant S 2014 Semiconductor metal oxides as hydrogen gas sensors *Procedia Engineering* **87** 795–802
- [3] Binions R and Naik A J T 2013 13 - Metal oxide semiconductor gas sensors in environmental monitoring ed R Jaaniso and O K Tan *Semiconductor Gas Sensors* (Woodhead Publishing) pp 433–66
- [4] Assadi M H N, Zhang Y, Zheng R K, Ringer S P and Li S 2011 Structural and electronic properties of Eu- and Pd-doped ZnO *Nanoscale Res. Lett.* **6** 357
- [5] Zhang T, Shen Y, Zhang R and Liu X 1996 Ammonia-sensing characteristics of Pt-doped CdSnO<sub>3</sub> semiconducting ceramic sensor *Mater. Lett.* **27** 161–4
- [6] Du Y, Gao S, Mao Z, Zhang C, Zhao Q and Zhang S 2017 Aerobic and anaerobic H<sub>2</sub> sensing sensors fabricated by diffusion membranes depositing on Pt-ZnO film *Sensors Actuators B* **252** 239–50
- [7] Haridas D and Gupta V 2012 Enhanced response characteristics of SnO<sub>2</sub> thin film based sensors loaded with Pd clusters for methane detection *Sensors Actuators B* **166–167** 156–64
- [8] Kang J G, Park J S and Lee H J 2017 Pt-doped SnO<sub>2</sub> thin film based micro gas sensors with high selectivity to toluene and HCHO *Sensors Actuators B* **248** 1011–6
- [9] Mhlongo G H, Motaung D E, Cummings F R, Swart H C and Ray S S 2019 A highly responsive NH<sub>3</sub> sensor based on Pd-loaded ZnO nanoparticles prepared via a chemical precipitation approach *Sci. Rep.* **9** 9881
- [10] Saito S, Miyayama M, Koumoto K and Yanagida H 1985 Gas sensing characteristics of porous ZnO and Pt/ZnO ceramics *J. Am. Ceram. Soc.* **68** 40–3
- [11] Siriwong C, Yimchoy J, Nabsanit S, Wisitsoraat A and Phanichphant S 2016 Hydrogen and ethanol sensing properties of Pd-loaded ZnO nanoparticles synthesized by flame spray pyrolysis *Advanced Materials Research* **1131** 146–52

- [12] Chou S, Teoh L, Lai W, Su Y and Hon M 2006 ZnO:Al thin film gas sensor for detection of ethanol vapor *Sensors* **6** 1420
- [13] Deshwal M and Arora A 2018 Enhanced acetone detection using Au doped ZnO thin film sensor *J. Mater. Sci.: Mater. Electron.* **29** 15315–20
- [14] Lu Y, Li J, Han J, Ng H T, Binder C, Partridge C and Meyyappan M 2004 Room temperature methane detection using palladium loaded single-walled carbon nanotube sensors *Chem. Phys. Lett.* **391** 344–8
- [15] Pradhan P and Ray A K 2005 A density functional study of the structures and energetics of small hetero-atomic silicon–carbon nanoclusters *J. Mol. Struct. THEOCHEM* **716** 109–30
- [16] Tonzzer M, Izidoro S C, Moraes J P A and Dang L T T 2019 Improved gas selectivity based on carbon modified SnO<sub>2</sub> nanowires *Frontiers in Materials* **6**
- [17] Claeysens F, Freeman C L, Allan N L, Sun Y, Ashfold M N R and Harding J H 2005 Growth of ZnO thin films—experiment and theory *J. Mater. Chem.* **15** 139–48
- [18] Hastir A, Kohli N and Singh R C 2016 Temperature dependent selective and sensitive terbium doped ZnO nanostructures *Sensors Actuators B* **231** 110–9
- [19] Li C C, Du Z F, Li L M, Yu H C, Wan Q and Wang T H 2007 Surface-depletion controlled gas sensing of ZnO nanorods grown at room temperature *Appl. Phys. Lett.* **91** 032101
- [20] Mitra P, Chatterjee A P and Maiti H S 1998 ZnO thin film sensor *Mater. Lett.* **35** 33–8
- [21] Zhu L and Zeng W 2017 Room-temperature gas sensing of ZnO-based gas sensor: a review *Sens. Actuators, A* **267** 242–61
- [22] Bhati V S, Hojamberdiev M and Kumar M 2020 Enhanced sensing performance of ZnO nanostructures-based gas sensors: a review *Energy Reports* **6** 46–62
- [23] Chaudhary S, Umar A, Bhasin K K and Baskoutas S 2018 Chemical sensing applications of ZnO nanomaterials *Materials (Basel)* **11**
- [24] Gholizadeh R, Yu Y-X and Wang Y 2017 N<sub>2</sub>O adsorption and decomposition over ZnO(0001) doped graphene: Density functional theory calculations *Appl. Surf. Sci.* **420** 944–53
- [25] Mhlongo G H, Motaung D E, Kortidis I, Mathe N R, Ntwaeaborwa O M, Swart H C, Mwakikunga B W, Ray S S and Kiriakidis G 2015 A study on the sensing of NO<sub>2</sub> and O<sub>2</sub> utilizing ZnO films grown by aerosol spray pyrolysis *Mater. Chem. Phys.* **162** 628–39
- [26] Yuan Q, Zhao Y-P, Li L and Wang T 2009 *Ab initio* study of ZnO-based gas-sensing mechanisms: Surface reconstruction and charge transfer *The Journal of Physical Chemistry C* **113** 6107–13
- [27] Alexiadou M, Kandyla M, Mousdis G and Kompitsas M 2017 Pulsed laser deposition of ZnO thin films decorated with Au and Pd nanoparticles with enhanced acetone sensing performance *Appl. Phys. A* **123** 262
- [28] Mhlongo G H, Motaung D E and Swart H C 2015 Pd<sup>2+</sup> doped ZnO nanostructures: Structural, luminescence and gas sensing properties *Mater. Lett.* **160** 200–5
- [29] Vinayan B P, Sethupathi K and Ramaprabhu S 2013 Facile synthesis of triangular shaped palladium nanoparticles decorated nitrogen doped graphene and their catalytic study for renewable energy applications *Int. J. Hydrogen Energy* **38** 2240–50
- [30] Cheng J, Hu D, Yao A, Gao Y and Asadi H 2020 A computational study on the Pd-decorated ZnO nanocluster for H<sub>2</sub> gas sensing: A comparison with experimental results *Physica E* **124** 114237
- [31] Kumar M, Singh Bhati V, Ranwa S, Singh J and Kumar M 2017 Pd/ZnO nanorods based sensor for highly selective detection of extremely low concentration hydrogen *Sci. Rep.* **7** 236
- [32] Zhang Y H, Yue L J, Gong F L, Li F, Zhang H L and Chen J L 2017 Highly enhanced H<sub>2</sub>S gas sensing and magnetic performances of metal doped hexagonal ZnO monolayer *Vacuum* **141** 109–15
- [33] Zhang Y H, Li Y L, Shen X R, Xie K F, Li T Y, Zhao J N, Jia Q J, Gong F L and Fang S M 2020 Rhombic ZnO nanosheets modified with Pd nanoparticles for enhanced ethanol sensing performances: An experimental and DFT investigation *J. Phys. Chem. Solids* **136** 109144
- [34] Liangruksa M, Sukpoonprom P, Junkaew A, Photaram W and Siriwong C 2021 Gas sensing properties of palladium-modified zinc oxide nanofilms: A DFT study *Appl. Surf. Sci.* **544** 148868
- [35] Kresse G and Hafner J 1993 *Ab initio* molecular dynamics for liquid metals *Physical Review B* **47** 558–61
- [36] Kresse G and Furthmüller J 1996 Efficient iterative schemes for *ab initio* total-energy calculations using a plane-wave basis set *Physical Review B* **54** 11169–86
- [37] Kresse G and Furthmüller J 1996 Efficiency of *ab-initio* total energy calculations for metals and semiconductors using a plane-wave basis set *Comput. Mater. Sci.* **6** 15–50
- [38] Kresse G and Hafner J 1994 Norm-conserving and ultrasoft pseudopotentials for first-row and transition elements *J. Phys.: Condens. Matter* **6** 8245–57
- [39] Perdew J P, Burke K and Ernzerhof M 1996 Generalized gradient approximation made simple *Phys. Rev. Lett.* **77** 3865–8
- [40] Grimme S, Antony J, Ehrlich S and Krieg H 2010 A consistent and accurate *ab initio* parametrization of density functional dispersion correction (DFT-D) for the 94 elements H-Pu *J. Chem. Phys.* **132** 154104
- [41] Grimme S, Ehrlich S and Goerigk L 2011 Effect of the damping function in dispersion corrected density functional theory *J. Comput. Chem.* **32** 1456–65
- [42] Henkelman G, Arnaldsson A and Jónsson H 2006 A fast and robust algorithm for Bader decomposition of charge density *Comput. Mater. Sci.* **36** 354–60
- [43] Tang W, Sanville E and Henkelman G 2009 A grid-based Bader analysis algorithm without lattice bias *J. Phys.: Condens. Matter* **21** 084204
- [44] Sanville E, Kenny S D, Smith R and Henkelman G 2007 Improved grid-based algorithm for Bader charge allocation *J. Comput. Chem.* **28** 899–908
- [45] Tusche C, Meyerheim H L and Kirschner J 2007 Observation of depolarized ZnO(0001) monolayers: formation of unreconstructed planar sheets *Phys. Rev. Lett.* **99** 026102
- [46] Freeman C L, Claeysens F, Allan N L and Harding J H 2006 Graphitic Nanofilms as Precursors to Wurtzite Films: Theory *Phys. Rev. Lett.* **96** 066102
- [47] Tu Z C and Hu X 2006 Elasticity and piezoelectricity of zinc oxide crystals, single layers, and possible single-walled nanotubes *Physical Review B* **74** 035434
- [48] Tu Z C 2010 First-principles study on physical properties of a single ZnO monolayer with graphene-like structure *Journal of Computational and Theoretical Nanoscience* **7** 1182–6
- [49] Shaw D 2013 *Introduction to Colloid and Surface Chemistry* (Elsevier, Butterworth-Heinemann)
- [50] Li S S 2006 *Semiconductor Physical Electronics* 2nd ed. (New York: Springer)
- [51] Li J H, Wu J and Yu Y X 2020 Theoretical exploration of single-layer Ti<sub>2</sub>O as a catalyst in lithium–oxygen battery cathodes *J. Phys. Chem. C* **124** 9089–98